JOURNAL OF APPLIED ELECTROCHEMISTRY **27** (1997) 1207–1211

$VSe_{2-y}S_y$ electrodes in lithium and lithium-ion cells

R. GUZMÁN, P. LAVELA, J. MORALES, J. L. TIRADO

Laboratorio de Química Inorgánica, Facultad de Ciencias, Universidad de Córdoba,
Avda. San Alberto Magno s/n, 14004 Córdoba, Spain

Received 11 November 1996; revised 20 January 1997

Step potential electrochemical spectroscopy data of lithium anode cells using $VSe_{2-y}S_y (0 \leq y \leq 0.5)$ compounds as cathode material and $LiClO_4$ solutions in PC as electrolyte were studied. On increasing y, a lower extension of the intercalation process was observed, due to the loss of a second insertion step corresponding to lithium ion occupancy of tetrahedral sites. In contrast, the reaction rate increased with sulfur content. $VSe_{2-y}S_y/LiCoO_2$ lithium-ion cells were cycled to test the electrochemical behaviour of the vanadium chalcogenides as anodic material. A better capacity retention was observed for $y = 0.3$. The effect of current density on the performance of the cells was also evaluated.

Keywords: *Lithium batteries, Lithium-ion batteries, Vanadium selenide, Vanadium sulfide*

1. Introduction

Rechargeable cells based in the lithium-ion concept are now considered to be the most promising batteries for modern portable appliances. As a result of the intermediate potential ranges of stability of their intercalation compounds as referred to lithium metal, first-row transition metal chalcogenides offer interesting possibilities as the electrode material for either lithium or lithium-ion cells [1].

1T-VSe_2(CdI_2-type structure) has been extensively studied as host lattice in chemical and electrochemical intercalation reactions. VSe_2 is unique among other layered transition metal dichalcogenides in showing a high c/a ratio which decreases on lithium insertion [2]. In addition, up to two lithium atoms per formula unit can be incorporated in the interlayer space of this chalcogenide by filling either octahedral or tetrahedral sites. Electrochemical lithium cells using Li_xVSe_2 as cathode material show reaction rates comparable with TiS_2 [3]. Moreover, two well defined steps were found to have equilibrium voltages almost independent of composition; these occur at around 2.0 V for $0 \leq x \leq 1$ and 1.3 V for $1 \leq x \leq 2$. More recently [4], it was shown that the lower molecular weight compositions $VSe_{2-y}S_y$ had similar galvanostatic discharge depths than VSe_2 for $0 < y \leq 0.8$, thus increasing the specific capacity and specific energy of the cells. However, discharges after the first plateau were not reported, as it was considered not to be useful for a cathode material.

Some of the electrochemical properties of $VSe_{2-y}S_y$, such as the reversibility of the intercalation reaction, make these systems potential candidates as electrode materials in lithium and lithium-ion cells. It should be noted that the use of similar solids, $SnSe_{2-y}S_y$, was recently reported in lithium and sodium cells [5]. Here we report the step potential electrochemical spectroscopy (SPES) and kinetic lithium insertion of $VSe_{2-y}S_y$. This study is complemented by the evaluation of the performance of $VSe_{2-y}S_y (0 < y \leq 0.5)$ as alternative anodes in lithium-ion batteries using $LiCoO_2$ as the positive electrode.

2. Experimental details

Four high-purity $VSe_{2-y}S_y$ powdered solids with $0 \leq y \leq 0.5$ compositions were obtained from the elements (Strem) in evacuated silica ampoules heated at 800 °C for seven days. Crystal growth and sample purification were achieved in a two-zone furnace with the cool end at 630 °C and the hot end at 700 °C by using Cl_2 as transport reagent: this was obtained *in situ* by the thermal decomposition of freshly prepared $(NH_4)_2PbCl_6$. $LiCoO_2$ was prepared from an intimate mixture of stoichiometric amounts of Li_2CO_3 and $Co(CH_3COO)_2$. The solids were heated for one day periods at the following temperatures; 400 °C, 600 °C and 900 °C with intermediate cooling-grinding steps. X-ray powder diffraction (XPD) was carried out using a Siemens D500 diffractometer with CuK_α radiation and a graphite monochromator.

The electrochemical behaviour of powdered sulfoselenide samples was evaluated in Li/Li-ClO_4(PC)/$VSe_{2-y}S_y$ cells. About 12 mg of pure compound were pressed against a 10 mg copper disc of 7 mm diameter. The resulting pellet had a thickness of active material (L) of about 0.07 mm and the copper substrate was maintained for the electrical contacts of the cell cathode. Step potential electrochemical spectroscopy [6] was carried out with a MacPile galvanostat–potentiostat system. A relaxation of the cells was allowed at the beginning of the experiment under open circuit conditions until $\Delta V/\Delta t$ was less that $1\,mV\,h^{-1}$. The spectra were recorded with –10 mV steps by measuring intensity relaxation at each voltage during the prefixed step duration (1 h) and calculating the average lithium content of the cathode material from the amount of electron charge transferred to the active material, on the assumption that no current flow was due to side reactions.

In lithium-ion cells, the vanadium dichalcogenide was assembled as anodic material and the oxide as cathodic material in three electrode cells with a lithium rod as the reference electrode. Both powdered active materials were mixed with 10% polytetrafluorethylene (PTFE) and 10% carbon black (Strem Chemical). The powdered mixtures were pressed at 3 tons on a stainless steel grid which acted as a support and electric contact. The electrolyte solution was a 1 M solution of $LiClO_4$ in 1 : 1 EC : PC mixture of the dehydrated solvents. The cell was connected to a MacPile galvanostat controlled by a MacIntosh computer. The experiments were set up in such a way that the chalcogenide anode was the working electrode. The voltage limits for the galvanostatic cycling experiments of lithium ion cells were those measured between $VSe_{2-y}S_y$ and the reference electrode (Li) in the three-electrode assembly. In order to use the capacity developed during the 2 V plateau, the abrupt variation of the voltage at the extremes of this plateau was used to control the cycle limits (1.8–2.2 V).

3. Results and discussion

The composition and unit cell parameters of pristine $VSe_{2-y}S_y$ solids are shown in Table 1. All XPD patterns could be indexed in the $P\bar{3}ml$ space group, in agreement with previous studies that define the composition limits of $1T\text{-}VSe_{2-y}S_y$ phases [4]. The c dimension and the unit cell volume decrease monotonically with y, while the decrease in a is within the experimental error. In addition, the I_{002}/I_{001} line intensity ratio decreases gradually with sulfur content as a consequence of the statistical distribution of an increasing number of low-scattering sulfur atoms in the 2c sites of the $P\bar{3}ml$ space group.

3.1. *Li/$VSe_{2-y}S_y$ cells*

As previously reported [2–4], the discharge curves of lithium cells using $VSe_{2-y}S_y$ cathodes recorded under experimental conditions close to the equilibrium show a first pseudo-plateau at around 2.0 V for $0 \leq x < 1$. This step has been described in terms of lithium intercalation into octahedrally coordinated sites. A second step at 1.3 V was found for $1 \leq x < 2$ in Li_xVSe_2, which was interpreted in terms of lithium insertion into tetrahedral sites [2, 3]. The occurrence of these successive steps during lithium intercalation into $VSe_{2-y}S_y$ electrodes was examined by plotting current relaxation against composition. Figure 1 shows two representative examples of the behaviour of this family of compounds. From the plot for $y = 0.1$ (Fig. 1(a)), a slow relaxation of the current was particularly evident in the vicinity of the first reduction peak, which is indicative of the slow diffusion of lithium ions in the interlayer space. The origin of the first effect is then attributable to V^{4+}/V^{3+} reduction accompanied by the progressive filling of octahedral sites by Li^+ ions. The broadening of the profile can be related to the presence of ordered intermediate phases such as those described by Thompson *et al.* [8] in Li_xTiS_2. The nature of the shoulder which develops for lithium contents larger than unity, may be ascribed to the filling of tetrahedral sites as found in VSe_2. However, the cell currents are low above

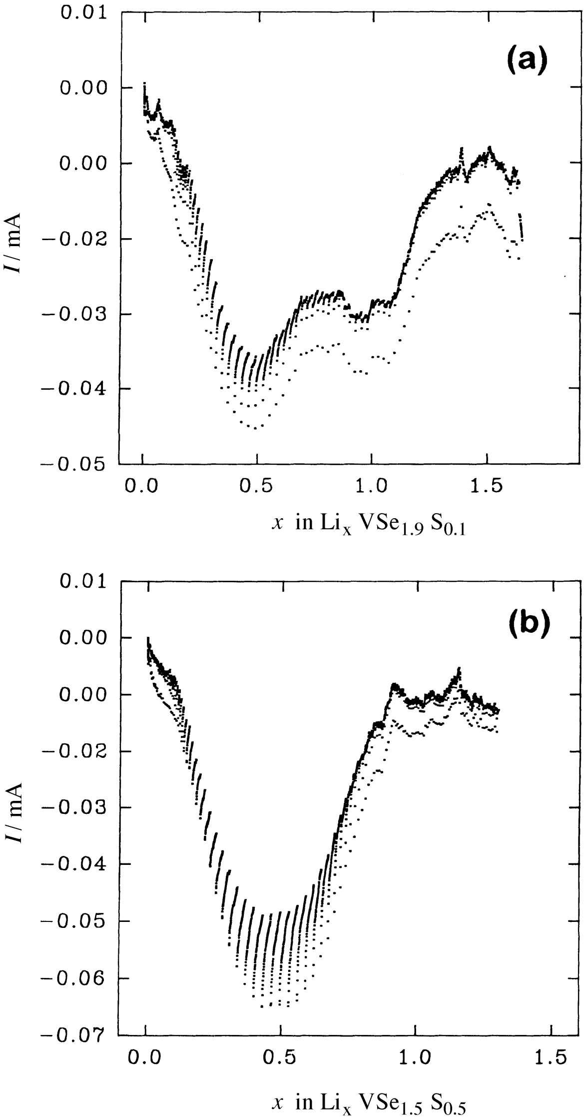

Fig. 1. Plot of current relaxation against composition for (a) $VSe_{1.9}S_{0.1}$ cells and (b) $VSe_{1.5}S_{0.5}$ cells.

Table 1. Composition and unit cell parameters of pristine $VSe_{2\text{-}y}S_y$

y in $VSe_{2\text{-}y}S_y$	a/Å	c/Å	V/Å^3	I_{002}/I_{001}
0.0	3.349_1	6.089_2	59.15	2.04
0.1	3.341_6	6.074_3	58.73	1.96
0.3	3.346_6	6.014_2	58.32	1.52
0.5	3.343_5	5.930_8	57.40	0.88

$x = 1.5$, thus indicating that the extent of intercalation above $x = 1$ is more limited for sulfur containing samples. This is particularly evident for $y = 0.5$ (Fig. 1(b)), for which the limiting composition is close to $x = 1$. In any case, none of these effects is attributable to electrolyte decomposition. Cyclic voltammograms of 0.1 M solutions of $LiClO_4$ in propylene carbonate with lithium metal and glassy carbon electrodes show that electrolyte reduction leads to significant currents only below 0.5 V, a behaviour also found by continuous cyclic voltammetry of these solutions [9].

Moreover, the absence of trailing current after the peak in Fig. 1(b) is indicative of a reversible process with limited extension, such as the complete filling of a particular set of sites by inserted Li^+ ions accompanied by V^{3+}/V^{2+} reduction. The peak voltage decreased slightly with sulfur content (2.0 V for $y = 0.1$ and 1.8 V for $y = 0.5$) which is indicative of the lower stability of an Li_2VS_2 phase as compared with Li_2VSe_2. In fact Li_2VSe_2 can be easily obtained by reaction of VSe_2 with *n*-butyllithium [2]. Concerning the fast relaxation of the current in the vicinity of the reduction shoulder shown in Fig. 1(a), its origin may be related to a rapid insertion of lithium ions in tetrahedral sites at the interlayer space which requires little expansion from the $LiVSe_2$ basal spacing (~0.005 nm).

In addition, the analysis of the relaxation plots may give evidence of the effects of selenium substitution on the rate of the lithium intercalation reaction in $VSe_{2-y}S_y$ electrodes. Figure 2 includes the current relaxation plots on a logarithmic scale for two selected potential steps recorded in the vicinity of the incremental capacity peak corresponding to the insertion of lithium ions in octahedral sites. The slope of $\log(|I|)$ against t is an indirect measurement of the rate of the lithium intercalation reaction. The larger value of slope found for the sulfur-rich composition (Fig. 2(b)) reveals the general behaviour found in these materials, in which an increase in the reaction rate with y is observed. This is probably as a consequence of the increasing ionic character of the lithium-chalcogenide bonds when the selenium atoms are substituted by less polarizable sulfur atoms. Less localized lithium–chalcogenide bonds favour the diffusion of the alkaline ions through the interlayer space.

According to the model described in [7], the diffusion coefficients show a direct relationship with the slope of $\log(|I|)$ against t plots when semiinfinite linear diffusion is assumed. This means that the relationship is not obeyed in a two-phase reaction defined at those composition ranges over which the voltage is invariant. According to the literature [3], the discharge curves of lithium cells using VSe_2 cathodes show two extended regions with almost constant voltage, which suggests a two-phase process. Thus, a quantitative evaluation of the diffusion coefficients from this data cannot be carried out in the regions over which the voltage is invariant. Lithium ion diffusion coefficients have been reported for $VSe_{2-y}S_y (0 \leq y \leq 0.3)$ in the 0.85–1.23 F mol^{-1} region in [4], which have the same order of magnitude as those computed from the slope of $\log(|I|)$ against t plots for $x = 0.85$–1.0 ($D \simeq 10^{-9} cm^2 s^{-1}$). These values of x are located far from the current peaks of the voltammogram and the regions of constant voltage in the discharge profile. Under these conditions, the slope is assumed to be $-1.071\, D L^{-2}$ [7].

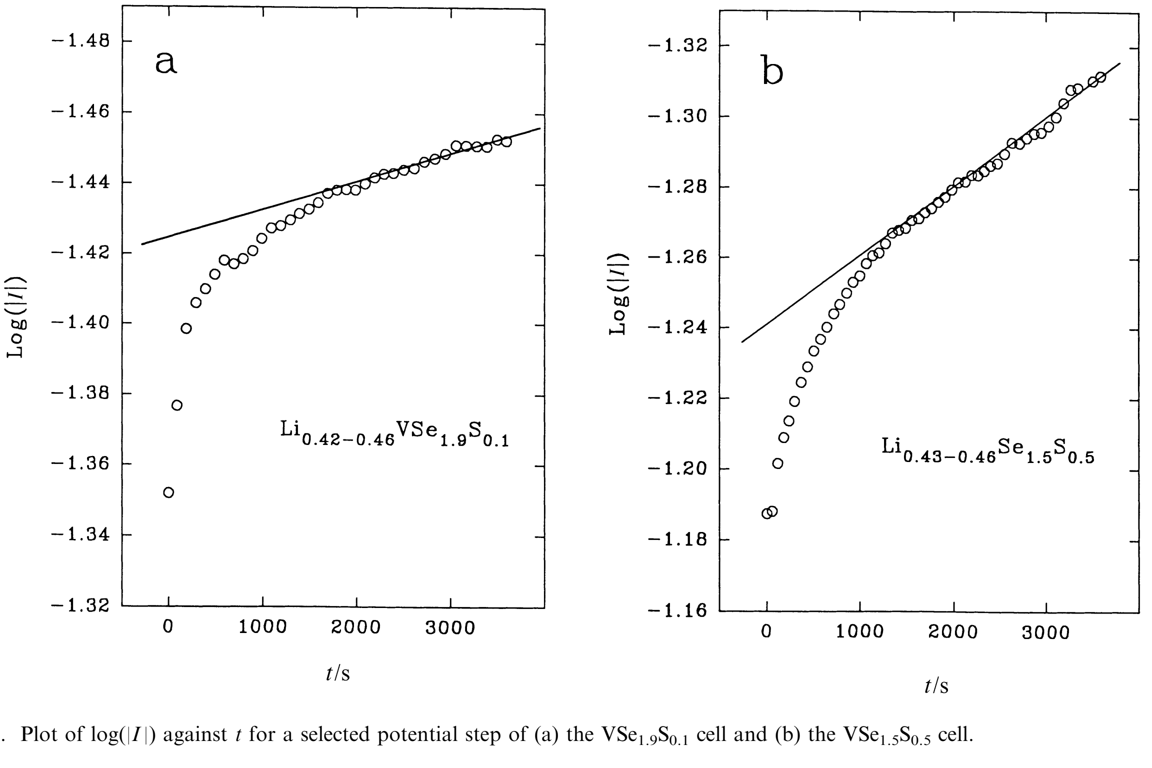

Fig. 2. Plot of $\log(|I|)$ against t for a selected potential step of (a) the $VSe_{1.9}S_{0.1}$ cell and (b) the $VSe_{1.5}S_{0.5}$ cell.

3.2. *Lithium-ion cells*

Lithium metal was used as the reference electrode while the chalcogenide was the negative electrode and the oxide was the positive electrode of the lithium-ion cells. The r^+/r^- mass ratio, as defined by the cathode active mass divided by the anode active mass, was initially established by assuming the following reaction:

$$2\,\mathrm{VSe}_{2-y}\mathrm{S}_y + 3\,\mathrm{LiCoO}_2 = 2\,\mathrm{Li}_{0.9}\mathrm{VSe}_{2y}\mathrm{S}_y + 3\,\mathrm{Li}_{0.4}\mathrm{CoO}_2 \qquad (1)$$

in which the filling of octahedral sites in the van de Waals interlayer of $\mathrm{VSe}_{2-y}\mathrm{S}_y$ only is assumed and a maximum of 0.6 lithium is allowed to be extracted from the oxide to avoid undesirable irreversible structural changes. However, several attempts to cycle the cells at the theoretical value ($r^+/r^- \simeq 0.7$) showed an enhanced polarization for a low number of cycles. Thus, mass ratios larger than the theoretical value ($r^+/r^- \simeq 1.5$) were used. Cell capacities will herein after be referred to the mass of active anode material.

Once the initial relaxation condition was fulfilled, the voltage measured between the anode and the cathode was close to zero. Henceforth, a previous charge of the cell by extracting lithium from the oxide electrode and inserting lithium into $\mathrm{VSe}_{2-y}\mathrm{S}_y$ was required. The maximum value of x in $\mathrm{Li}_x\mathrm{VSe}_{2-y}\mathrm{S}_y$ reached during cell charge was always lower than unity. This agrees with an exclusive occupancy of the octahedral sites located at the interlayer space. As $\mathrm{VSe}_{2-y}\mathrm{S}_y$ ($y < 0.5$) may incorporate more than one lithium per formula by occupancy of tetrahedral sites in the interlayer space, this material is particularly interesting in lithium-ion cells, as it may allow overcharge phenomena without cell electrolyte damage, provided that the cathode material exceeds the stoichiometric value in Equation 1.

To evaluate the effect of the composition of the anodic material, different cycling experiments were carried out under the same current density (120 μA cm^{-2}) and mass ratio, by changing the value of y in $\mathrm{VSe}_{2-y}\mathrm{S}_y$. Figure 3 compares the behaviour observed during the first 50 cycles for $y = 0.3$ and 0.5. A significant loss of capacity is caused by the extended substitution of Se atoms by S atoms in the host chalcogenide lattice, although capacity retention is comparable for both compositions.

Additional experiments were carried out in order to determine the influence of current density on the capacity for the $\mathrm{LiCoO}_2/\mathrm{VSe}_{1.7}\mathrm{S}_{0.3}$ cell by maintaining $r \simeq 1.5$. The capacity versus number of cycles plots at different intensities are also displayed in Fig. 3. A maximum in cell capacity is detected for 180 μA cm^{-2}. Increasing the current parameter density over this value does not give an increase in capacity. This limiting value is probably imposed by the finite value of the diffusion coefficients of lithium ions in the chalcogenide electrodes. After the first cycle a slight, but significant, increase in capacity is observed from cycle 2 to 10, which is followed by small changes in capacity up to 50 cycles. Finally, the charge–discharge curves obtained for the most favourable composition/conditions are shown in Fig. 4. The shape of the charge and discharge profiles suffer little change during the complete experiment.

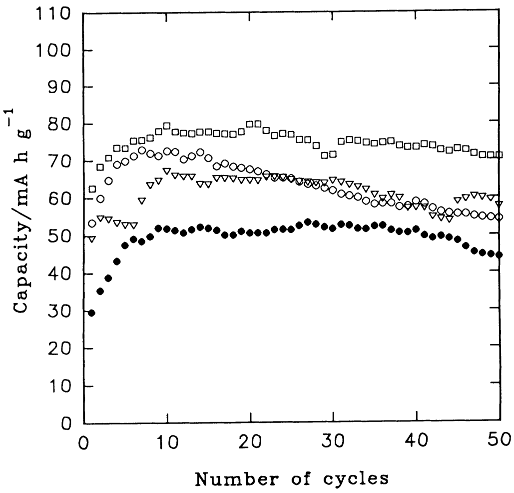

Fig. 3. Cell capacity against cycle number for the $\mathrm{LiCoO}_2/\mathrm{VSe}_{2-y}\mathrm{S}_y$ ($y = 0.3, 0.5$) lithium-ion cells. Key: (●) $y = 0.5$, 120 μA cm^{-2}; (○) $y = 0.3$, 120 μA cm^{-2}; (□) $y = 0.3$, 180 μA cm^{-2}; (▽) $y = 0.3$, 240 μA cm^{-2}.

4. Conclusions

The use of $\mathrm{VSe}_{2-y}\mathrm{S}_y$ compounds as electrode material for rechargeable batteries offers interesting opportunities. The general trend can be summarized as follows: (i) with increasing y the molecular weight of the solid decreases, thus increasing the specific capacity and specific energy of cells containing these materials as active components; (ii) high sulfur contents cause a lower extension of the intercalation process due to the loss of the second insertion effect at lower voltages; (iii) in addition, the rate of the lithium intercalation reaction increases with sulfur content.

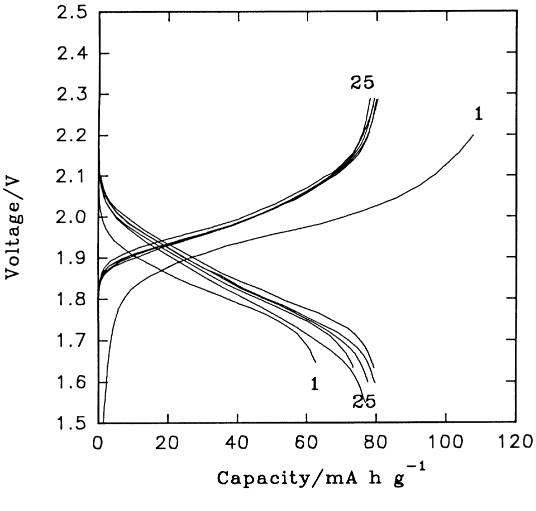

Fig. 4. Charge/discharge profiles for the $\mathrm{LiCoO}_2/\mathrm{VSe}_{1.7}\mathrm{S}_{0.3}$ lithium-ion cell cycled at 180 μA cm^{-1}.

Taking into account the chemical potential ranges of insertion compounds relative to lithium metal and the kinetics of lithium intercalation into the different compounds investigated here, the use of layered $VSe_{2-y}S_y$ compounds as anode materials (e.g., against Li, Co oxide cathodes) can be considered an interesting option. The evaluation of $VSe_{2-y}S_y$ anodes for these purposes shows good cycling performance of the resulting cells, particularly for $y = 0.3$. Cell performance is improved by increasing the intensity through the cell up to 180 μA cm^{-2} and increasing the mass ratio to 1.5, which leads to capacity values close to 70 mA h g^{-1} after 50 cycles.

Acknowledgement

This work was supported by the CEC Joule Program Contract no. JOU2-CT93-0326 and CICYT MAT94-1155-CE and MAT93-1204.

References

[1] E. J. Plichta and W. K. Behl, *J. Electrochem. Soc.* **140** (1993) 46.

[2] M. S. Whittingham and F. R. Gamble, *Mater. Res. Bull.* **10** (1975) 363.

[3] *Idem, ibid.* **13** (1978) 959.

[4] F. Dalard, D. Deroo, A. Sellami, R. Mauger and J. Mercier, *Solid State Ionics* **2** (1981) 321.

[5] J. Morales, C. Pérez-Vicente, J. Santos and J. L. Tirado, *Electrochim. Acta* **42** (1997) 257.

[6] Y. Chabre, *J. Electrochem. Soc.* **138** (1991) 329.

[7] C. J. Wen, B. A. Boukamp, R. A. Huggins and W. Weppner, *ibid.* **126** (1979) 2258.

[8] A. H. Thompson, J. C. Scanlon and C. R. Symon, *Solid State Ionics* **1** (1980) 47.

[9] M. Arakawa and J. I. Yamaki, *J. Electroanal. Chem.* **219** (1987) 273.